Static microdroplet arrays: a microfluidic device for droplet trapping, incubation and release for enzymatic and cell-based assays†

Ansgar Huebner,[ab] Dan Bratton,[b] Graeme Whyte,[b] Min Yang,[bc] Andrew J. deMello,[d] Chris Abell[b] and Florian Hollfelder*[a]

Received 7th August 2008, Accepted 14th October 2008
First published as an Advance Article on the web 27th November 2008
DOI: 10.1039/b813709a

We describe the design, fabrication and use of a single-layered poly(dimethylsiloxane) microfluidic structure for the entrapment and release of microdroplets in an array format controlled entirely by liquid flow. Aqueous picoliter droplets are trapped en masse and optically monitored for extended periods of time. Such an array-based approach is used to characterize droplet shrinkage, aggregation of encapsulated *E. coli* cells and enzymatic reactions. We also demonstrate that trapped droplets may be recovered from the microfluidic array for further processing.

Introduction

Array-based technologies have broad applications in drug discovery, microbiology and cell biology.[1] The high density and small scale of arrayed reactors allows for parallel processing and monitoring of chemical and biological assays using small amounts of liquid. Such systems range from 96-well microtitre plates to high-density microarrays.[2] Current developments in this field are directed towards further reductions in sample volumes, increasing analytical throughput and integration of pre- and post assay processing. Nanolitre drop dispensers such as nanopipettes[3,4] are promising examples in this regard.

Recent developments in chip-based microfluidics provide a facile route to harnessing the inherent benefits of system miniaturization.[5] A variety of microfluidic systems for trapping micron-sized beads or cells for single cell studies have been described. These are typically based on the idea of reducing the well volumes in a standard microtitre plate from tens of microlitres to the nano- or picolitre scale.[6–9] However, one key disadvantage associated with conventional microfluidics is the requirement that individual experiments are spatially separated in discrete chambers to prevent interactions or cross-contamination between individual assays. Microdroplet-based systems provide one solution to this problem: the microdroplet compartment acts as an independent, spatially separated reactor.[10–12] Microfluidic droplets are normally aqueous, have a volume ranging from a picolitres to nanolitres, are surrounded and isolated by a continuous oil phase and can be generated at kHz frequencies with precise control over their size and polydispersity.[13,14] Droplets can be incubated[15–18] and manipulated by splitting,[19] fusion,[20–22] sorting,[20,22–24] cooling[25] or heating.[26]

Microfluidic droplets have already proven a useful experimental paradigm in biology and chemistry, and have been applied to *in vitro* protein expression,[15,17] fast enzymatic[27,28] and cell-based assays,[29–31] PCR reactions,[32] protein crystallization,[33,34] DNA binding assays[35] and the detection of protein expression in cells.[36]

In this study we present a device that enables local storage and release of picoliter-sized water-in-oil droplets without the use of electrical or optical actuators. A single layer poly(dimethylsiloxane) (PDMS) device (Fig. 1) was used to generate, store, incubate, monitor and isolate droplets. The versatility of this system was demonstrated by monitoring cell behaviour and detecting enzymatic turnover within such droplets. In each case the process of droplet trapping provides a scaled-down version of a standard laboratory instrument, reducing the assay scale to a few picoliters for each reaction.

Materials and methods

Device fabrication

All microfluidic devices were constructed using conventional soft lithographic techniques.[37,38] Briefly, a master was prepared from an SU 8 2025 (Microchem Corp.) coated silicon wafer (Compart Technology Ltd.) to yield features 50 μm in height. To form structured microfluidic substrates Sylgard 184 (Dow Corning) was mixed in a 10:1 (w/w) ratio of resin to crosslinker and then poured over the master. After degassing, the device was cured for six hours at 65 °C. The cured PDMS was cut and peeled off the master. Access holes for fluidic tubing were created using a biopsy punch, and the device exposed to an air plasma (Femto Diener) for 30 seconds followed by sealing to a glass microscope slide (Agar Scientific). The channels were then rendered hydrophobic by baking at 65 °C for 10–12 hours before use. Polyethylene tubing (internal diameter ID = 308 μm, Beckman

[a]*Department of Biochemistry, University of Cambridge, 80, Tennis Court Road, Cambridge, UK CB2 1GA. E-mail: fh111@cam.ac.uk; Fax: +44 1223-766002; Tel: +44 1223-766048*
[b]*Department of Chemistry, University of Cambridge, Lensfield Road, Cambridge, UK CB2 1EW. E-mail: ca26@cam.ac.uk; Fax: +44 1223 336362; Tel: +44 1223 336405*
[c]*The School of Pharmacy, University of London, Brunswick Square, London, UK WC1N 1AX*
[d]*Department of Chemistry, Imperial College London, South Kensington, London, UK SW7 2AZ*
† Electronic supplementary information (ESI) available: Details of protein production, data traces for kinetic measurements of several static droplets, raw data traces for multiple arrays, description of the movie showing release of droplets. See DOI: 10.1039/b813709a

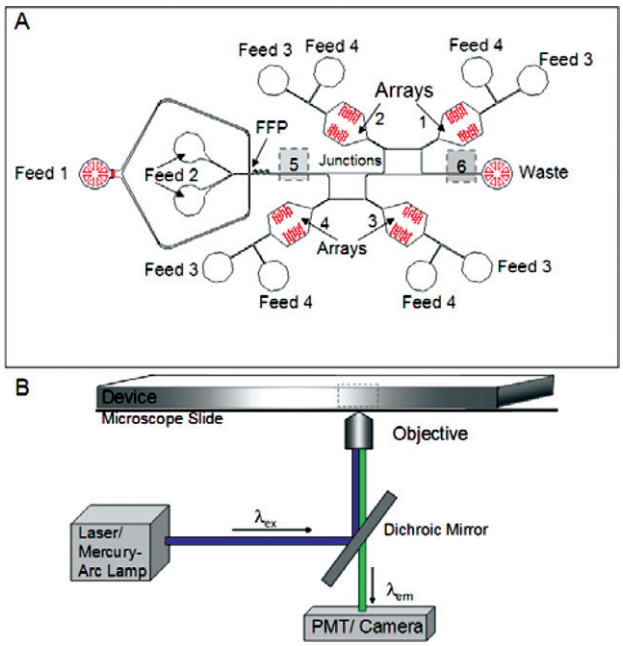

Fig. 1 (A) Design of a four-trap array microfluidic device allowing droplet generation, entrapment, incubation, monitoring and release. Droplet formation occurs at a flow focusing point (FFP) where two oil streams (originating from Feed 1) enter perpendicularly to an aqueous stream (originating from Feed 2). Once the system has equilibrated, droplets are directed into a trap array by withdrawing oil from Feed 3 (Feed 3 and Feed 4 describe inlets with the same function for all four arrays). Reversal of the oil flow from the same Feed 3 was used to avoid deposition of initial, polydisperse droplets generated before droplet formation had stabilized. These droplets were sent to the waste. The trap arrays 1–4 could be filled by withdrawing oil from Feed 3. Droplets deposited in traps were monitored by placing the device onto a microscope equipped with a camera for bright-field or fluorescence visualization (see 1B). Positions for laser-induced fluorescence measurements are indicated by the grey shaded boxes (A). The shaded box labelled 5 corresponds to t = 0 sec, and the shaded box labelled 6 to time points after release of droplets. Droplets were released at specific time points by injecting oil from Feed 4. The device contains four arrays each comprising 96 traps and can accommodate a total of 384 trapped droplets. (B) Droplets were analyzed using a microscope set-up operating in two different modes. Firstly a mercury-arc lamp was used to excite the entire array and the fluorescence emission was recorded with a fluorescent camera. Secondly, for laser-induced fluorescent measurements a laser was used and the emitted light was detected with a photo-multiplier tube (PMT). In both systems a dichroic filter system was used to remove any residual excitation light.

Dickinson) was used to interface to glass syringes containing reagents (Hamilton).

Device operation and droplet formation

Hydrodynamic fluid flow was generated and controlled by syringe pumps (Harvard Apparatus PhD 2000). Light mineral oil (Sigma Aldrich) containing 1–2% (w/w) Span 80 (Fluka) as a stabilizer was used as the immiscible oil phase. All liquids were filtered prior to use with a filter cartridge (0.22 μm, Millex®GP, Millipore). Droplets were generated using a flow focusing device (FFD) element,[39] with either one or two aqueous inlets delivering droplets that approximately correspond to the 50 μm diameter of the traps. In all experiments the water fraction[40] was kept at a constant value of 0.25. Droplets were stored under a constant flow rate of 0 or 1 μL/hr.

Droplet imaging

Droplets within the trapping array were imaged using an inverted microscope (IX71, Olympus). A Phantom V7.2 camera was used to record images at 100 frames per second in bright-field mode. Alternatively an EMCCD camera (XonEM$^+$ DU 897, Andor) was coupled to the microscope to visualize fluorescent cells or molecules within individual droplets. The device was illuminated using a 100 W mercury arc-lamp (U-RFL-T, Olympus). A filter cube (UMWIB, Olympus) was used to remove any residual excitation light. To minimize fluorophore photobleaching a neutral density filter (ND50, Olympus) and a shutter (Lamda-SC, Sutter Instruments) synchronized to open for 200 ms during each measurement event were installed. Both camera and shutter were controlled with LabView®8.2 software (National Instruments).

Laser-induced fluorescence measurements were conducted by placing the microfluidic device on the microscope coupled with a diode-pumped solid state laser excitation source (Piccaro 488 nm air-cooled cyan). A microscope objective (10x UPlanFLN, Olympus) was used to focus the excitation light within the microfluidic channel. The voltage output of the photomultiplier tube (H8249, Hamamatsu) was recorded and fed into a computer *via* a National Instruments acquisition card (PCI 6251) and processed using LabView®8.2.

Cell assay

An *E. coli* cell culture was prepared by inoculating 4.0 mL of a fresh Luria–Bertani broth (LB medium) containing ampicillin (200 μg/mL) with 40 μL of an overnight culture of *E. coli* BL21(DE3) that was transformed with the plasmid harbouring mRFP1[41] in a pIVEX construct. After incubation (16 h, 25 °C, 225 rpm) cells were spun down (15 min at 5000 rpm), resuspended in fresh LB medium and spun down again. This procedure was repeated twice to remove small cell particles and free proteins. Cells were resuspended in LB to a density of $A^{600nm} = 1.0$. This resulted in most droplets containing between seven and ten cells.

Droplet stability

To characterize droplet shrinkage as a function of the oil flow rate (mineral oil containing Span 80 1.5%, w/w), droplets were formed containing 100 μM yellow fluorescent protein (Venus). For each oil flow-rate a volume shrinking factor (see Results & Discussion) was fitted using KaleidaGraph software (Synergy Software).

Enzymatic assays

To monitor enzymatic hydrolysis, galactosidase (300 nM) was co-encapsulated with substrate at 80 μM or 200 μM, which in bulk solution was converted fully in 15 and 45 minutes, respectively (data not shown). Time-integrated fluorescence signals were adjusted to compensate for droplet shrinkage.

Results and discussion

Loading traps with droplets

Droplets with a diameter of approximately 50 μm were formed using a standard flow focusing geometry[39,42] and deposited in the integrated trap structures shown in Fig. 1. Two oil streams (from Feed 1) merge perpendicularly to the aqueous stream (from Feed 2). An oil stream is introduced from Feed 4 to prevent any droplets from entering the array during the initial stabilization stage. Once droplets are of uniform size, the oil flow from Feed 4 is reversed resulting in the entrapment of droplets in the array.

A rapid channel expansion at the entrance of the array ensures a fast and homogenous proliferation of droplets into the trap array. To ensure that only one droplet enters each trap an exhaust channel was structured through the centre (Fig. 2).

Accordingly, when a trap is empty, oil is able to flow through this exhaust channel. However, as soon as a droplet is captured it blocks the exit resulting in the termination of liquid flow within the trap and preventing a second droplet from entering the trap. Since most droplets (>90%) pass through the array chamber without being trapped, the structure is ideal for randomly sampling a defined subset of a large droplet population. This concept is analogous to the approach reported by DiCarlo *et al.* for trapping populations of single cells in a microfluidic array albeit without using emulsion droplets.[7]

Once each array is filled with droplets (as shown in Fig. 2), all inlets except Feed 1 are closed to maintain this arrangement. This procedure ensures reliable control of oil flow from Inlet 1 throughout the trap array into Feed 4. After the trapped droplets have been incubated for a given period of time they can be released by supplying a fresh oil flow from Feed 4. After flow reversal, droplets occasionally got stuck at the rear side of the adjacent trap. Therefore the shape of the trap backside (characterized by the angle alpha, shown in Fig. 2A) was slightly altered to ensure smooth passage of droplets leaving the device after flow reversal: A change of this angle from 90° to 110° resulted in an increase in droplet recovery from 70% to > 90%

Cell encapsulation

Immobilizing aqueous droplets in the described manner allows facile monitoring of encapsulated cells over extended periods of time. In the current studies bacterial cells (1 to 2 μm in diameter) were encapsulated within such trapped droplets, and their interactions and movement were monitored over a period of 15 minutes. For easy visualization *E. coli* cells expressing red fluorescent protein (from plasmid mRFP1)[41] were encapsulated within droplets. Fig. 3 illustrates a trapped droplet containing seven cells. It can be seen that the encapsulated cells begin to aggregate after a few minutes. Control experiments with fewer cells per droplet (two to three cells) and fluorescent beads did not show any aggregation events (data not shown). These observations suggest that aggregation is favoured at higher densities of *E. coli* cells and is likely a result of oxygen depletion. This effect has been described previously in the literature.[43] The combination of the ability to tailor the number of cells in a droplet by dilution[36] or to change variables such as pH and salt concentration with the ability to subsequently monitor a cell's response will be highly desirable in facilitating an understanding of basic phenomena at the single cell level and the behaviour of populations of cells.[30] The encapsulation of single cells has been demonstrated previously,[18,29,44] but here we show that such a set-up allows information about the morphological behaviour of a population to be obtained simultaneously with the optical readout from each single bacterial cell.

Droplet stability and long-term droplet storage

When conducting reactions in a defined reactor it is important to be able to maintain the reaction volume or to be able to

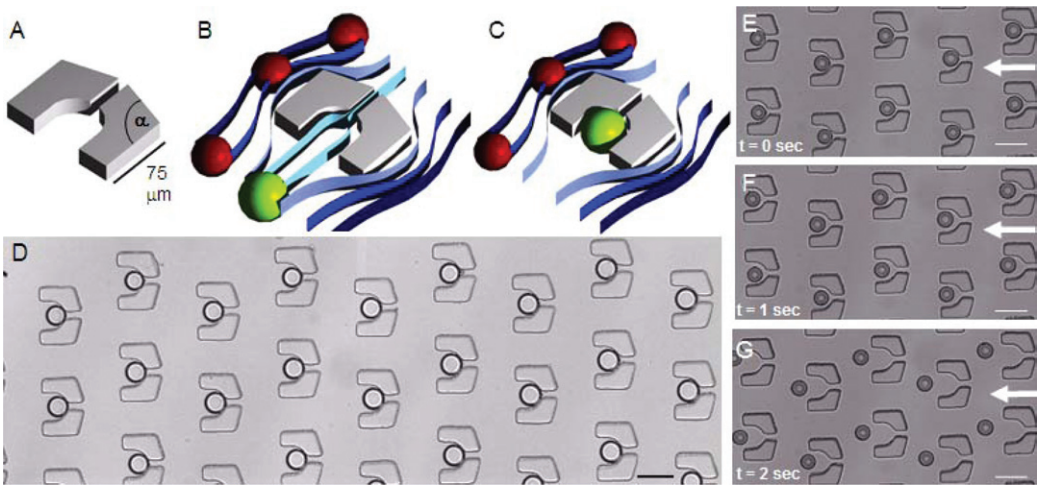

Fig. 2 Droplet trapping arrays. (A) Design of an individual trap (with a scale bar indicating the dimensions) The rear of the trap was drawn to give a 110° angle (α). This improved the percentage rate of droplets that could be retrieved from an array to above 90%. (B) Schematic flow profile for droplets approaching a trap. Liquid enters through the opening in the centre of the trap. (C) Schematic flow profile when a droplet is residing in the trap. As soon as a trap is occupied by a droplet, additional droplets pass outside the trap. This mechanism ensures that only a single droplet is trapped per feature. (D) Image of an array containing uniformly trapped aqueous droplets. (E)–(G) Brightfield images of droplet release over a 2 second time period. The direction of flow is indicated by the white arrows. Figures A–C are not drawn to scale. *Conditions*: Aqueous droplets were formed from buffer (PBS at pH 7.4) in light mineral oil and 1.5% (w/w) Span 80. Scale bars indicated in the bottom right corner of each image correspond to a distance of 75 μm.

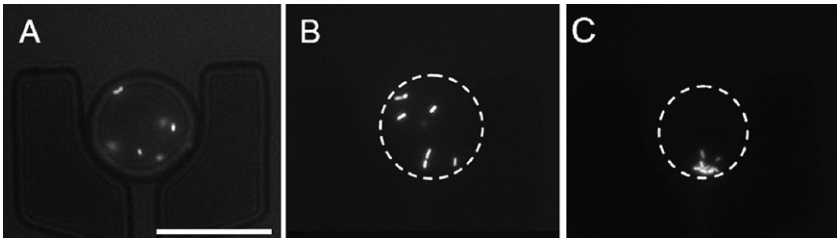

Fig. 3 Monitoring aggregation of encapsulated *E. coli* cells. *E. coli* cells harbouring red fluorescent protein (mRFP1) as a marker were encapsulated in aqueous droplets formed in light mineral oil and 1.5% (w/w) Span®80. Images demonstrate that it is possible to monitor cell movement in a trapped droplet. After initial encapsulation the cells moved and eventually aggregated (as shown in panel C): (A) fluorescence image at t = 0 minutes (with brightfield overlay); (B) at t = 2 minutes and (C) at t = 15 minutes (fluorescence only). Images were taken with a 40x objective, an ND 50 filter and a 50 ms exposure. Dotted lines in (B) and (C) describe the position of the droplet in the absence of an overlay with the brightfield image (as in A). The scale bar in A represents 50 μm. The oil flow rate was 0 μL/h.

characterise any volume variations. This ensures extraction of the true amount of reagents or products. When working with a biphasic system it is possible that one of the liquid phases may partition into the other, thus changing the volume of the droplet. To assess whether immobilized droplets maintain their volume over extended periods of time, trapped droplets containing a yellow fluorescent protein (YFP, 'Venus'[45]) were studied using epifluorescence microscopy. This protein was chosen as a probe since it possesses a low photodegradation rate coefficient, has a high fluorescence quantum efficiency,[45] and, unlike hydrophobic small molecules, does not leak out of the water phase. Fig. 4(A–F) shows clear evidence of droplet shinkage over 50 minutes. Accordingly, and since YFP does not photobleach or leak out of the discontinuous phase, the measured fluorescence intensity increase as the droplet shrinks (Fig. 4(G)).

To quantify the observed volume decreases, a droplet shrinking factor (V_F) was defined as,

$$V_F(t) = \frac{F(t_0)}{F(t_x)} \quad (1)$$

and used to characterize the shrinking process. $F(t_0)$ defines the fluorescence intensity of the droplet at $t = 0$ and $F(t_x)$ defines the fluorescence intensity at a time point t = x minutes. Fig. 4(G) shows V_F as a function of time for various volumetric flow rates of the continuous-phase. Qualitatively this variation follows an exponential decay model. Such behaviour can be explained using a simple model in which the loss of water from the droplet is related to the surface area exposed to the oil phase. In other words, a smaller surface area reduces water loss and thus decreases the droplet shrinking rate. The change in surface area as a function of time can be described using,

$$\frac{\Delta S}{\Delta t} = -k \times S \quad (2)$$

Here S is the surface area, k is a constant of proportionality and t is time. As the change in surface area is proportional to the change in volume, integration of equation 2 delivers,

$$V_F(t) \propto S(t) = A\exp(-kt) \quad (3)$$

where A is a pre-exponential factor and k is the shrinking rate factor. This model is in good qualitative agreement with our data, although a more complicated scenario cannot be excluded.[46,47] Individual shrinkage curves could be fit to a single exponential decay, suggesting that this treatment provides an empirical way of quantifying droplet shrinkage. Furthermore, the rate of shrinkage is proportional to the oil flow rate, *i.e.* a faster rate of droplet shrinkage for higher oil flow rates was observed. This is consistent with a model in which a larger amount of water partitions more readily into the oil phase when this phase is renewed more quickly.

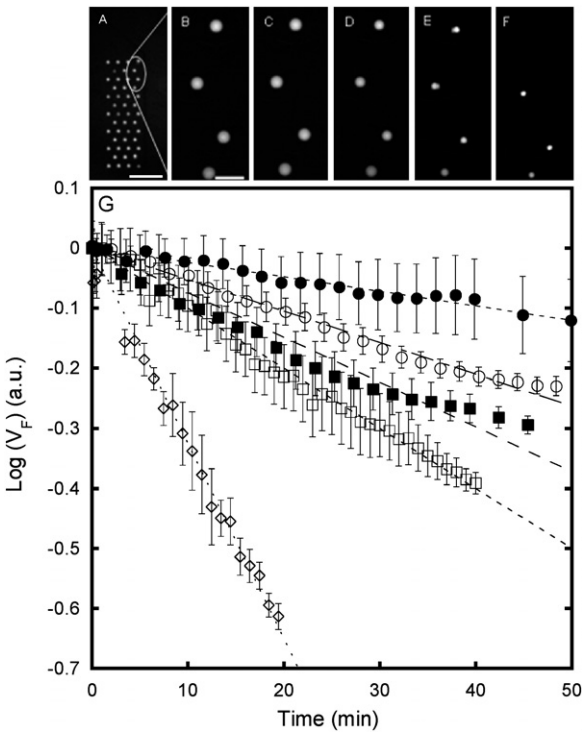

Fig. 4 Assessment of droplet shrinkage as a function of time. (A) Droplets containing yellow fluorescent protein (YFP) were trapped in the array and viewed under a 2x objective. (B–F) Images of four droplets recorded at different times with a 40x objective, (B) t = 0, (C) t = 1 min, (D) t = 10 min, (E) t = 30 min, and (F) t = 50 min. A constant flow rate (10 μL/h) of light mineral oil with 1.5% Span 80 (w/w) was maintained throughout the experiments shown in panels B–F. (G) reports the variation of the volume shrinking factor (V_F) as a function of different oil flow rates based in the readout of the droplets [100 μL/h (◇), 10 μL/h (□), 5 μL/h (■), 1 μL/h (○) and 0 μL/h (●)]. The error bars represent the standard deviation of V_F resulting from the analysis of the data obtained from all droplets. The scale bar in (A) is 600 mm and 100 mm in (B–F).

Enzymatic assay

In order to explore the potential of the trapping device with regard to measuring a kinetic process, a simple enzymatic assay was conducted. Microdroplet-based microfluidic devices have been shown to be useful tools in extracting kinetic information from such processes by analyzing moving droplets along an extended channel.[27,31] However, assay timescales are limited by the time the droplet remains within the microfluidic device. The channel length in turn is defined by back pressure limitations. To show that the droplet arrays can aid in studying processes on extended timescales, the β-galactosidase from *Sulfolobus Sofataricus* (SsβG) was co-encapsulated with the fluorogenic substrate fluorescein-mono-galactoside (FMG) using a FFD with two aqueous inlets. The kinetics of multiple (discrete) droplets were measured simultaneously over a period of more than 40 minutes.

The enzymatic reaction (Scheme 1) was followed simultaneously over time in multiple droplets. The recorded intensity data were corrected for droplet shrinkage at a constant oil flow of 1 μL/hr (data taken from Fig. 4(G)). The resulting time courses shown in Fig. 5 are well correlated and in good agreement with analogous measurements made in bulk (data not shown).

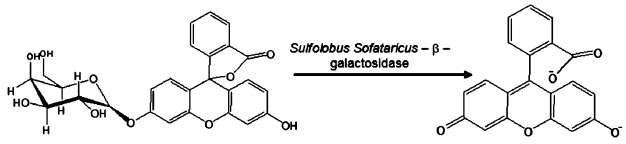

Scheme 1 The enzymatic reaction followed in time-resolved measurements.

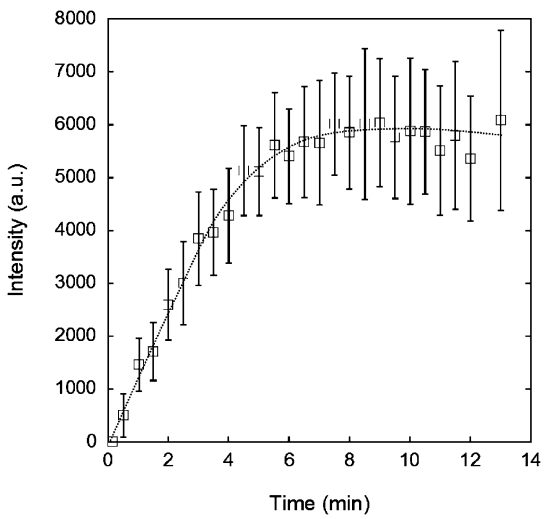

Fig. 5 Time course of an enzymatic reaction within trapped droplets. The average fluorescence intensity of multiple entrapped droplets was monitored simultaneously using an EMCCD camera (XonEM$^+$ DU 897, Andor) over a period of 15 minutes. The dotted line is merely to guide the eye. Data were corrected for droplet shrinkage (see Fig. 4). The data traces used to derive this Figure are shown in the ESI (S1)†. *Conditions*: [ssbGal] = 300 nM; [FMG] = 80 μM. 24 °C, pH 6.4, 1 μL/h oil flow.

Release of droplets

An instrumental format for performing complex biochemical reactions ideally involves the storage and release of droplets at a variety of timepoints. Droplets should ideally be stored, monitored, and then released after different incubation times. Accordingly, efficient droplet recovery in our system will allow for more complex experiments involving longer incubation times and modification or isolation of individual droplets. Here we demonstrate that recovery of droplets enable a laser spectroscopic setup to measure the progress of the kinetic reaction. This procedure was exemplified for the enzymatic reaction shown in Scheme 1.

Droplets containing ssβGal [300 nM] and FMG [200 μM] were deposited in all reservoirs simultaneously (384 droplets in total). Once the arrays were fully occupied, oil flow was terminated and droplets left to incubate.

After different time intervals (5, 10, 20 and 40 minutes) droplets were released from each array by applying an oil flow from Feed 4 (Fig. 1). When the flow was reversed droplets were flushed back into the channel area (see http://www-microdroplets.ch.cam.ac.uk/research/movies/trap.html for a movie†) Data were corrected for droplet shrinkage and found to be in good agreement with bulk measurements where the substrate was consumed in 45 minutes (Fig. 6). Measurement of the fluorescence signal of each droplet at the exit of the device (Fig. 1–area 6) indicated that more than 90% of droplets (*i.e.* 90 out of 96) could be released from each reservoir and analyzed afterward.

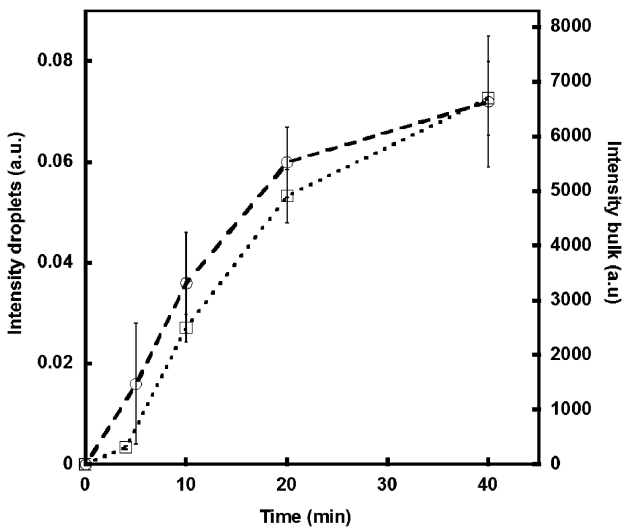

Fig. 6 Time course of an enzymatic reaction measured after release of droplets. Variation of laser induced time-integrated fluorescence intensity as a function of time for the enzymatic reaction of ssβGal [300 nM] with fluorescein-mono-galactoside (FMG) [200 μM]. Data obtained from the analysis of droplets (○) and bulk solution (□) are shown. For droplet measurements time points stem from the average photon counts of droplets that were released after incubation for a given period of time in a reservoir. Error bars indicate the spread of fluorescence counts for approximately 90 droplets and the standard deviation from bulk experiments (measured three times) at each time point. Data for the droplets were compensated for droplet shrinkage. The raw data used to derive this Figure are shown in the ESI (S2).† *Conditions*: 24 °C, pH 6.4, 1 μL/h oil flow.

Conclusions

The simple microfluidic array reported here can be used to trap and monitor hundreds of aqueous picoliter droplets simultaneously. Droplets can be trapped, incubated and retrieved at will without the use of electric circuits, lasers or valves, significantly reducing the complexity of fabricating such a device.

A simple empirical correction can be applied to account for oil-flow dependent shrinkage of droplets resting in the trapping arrays. This correction makes it possible to obtain time courses in which product formation by encapsulated enzyme or enzyme-producing cells are measured in a quantitative fashion.

Additionally, more complex systems involving enzymatic reactions and cell behaviour have been investigated. A population of seven *E. coli* cells was encapsulated within a droplet and cell aggregation monitored in real time. As previously noted, the ability to tailor the number of cells in a droplet or variables such as pH and salt concentration combined with the ability to subsequently monitor a cell's response allows basic phenomena at the level of few (or single) cells to be probed with great sensitivity. Indeed, the droplet array allows the simultaneous immobilisation of several droplets and thus provides a route to extracting quantitative information on individually compartmentalised ensembles with statistical redundancy.[30]

The demonstration that enzymatic reactions within droplets can be conveniently monitored in a trap array by a microscopic camera, shows that miniaturised assays are possible. For smaller amounts of product or less fluorescent reaction products the sensitivity of the camera will determine the detection limits of the assay. If higher sensitivity is required, *e.g.* for the characterization of slower enzymes and in directed evolution, where initial activities in libraries are often initially marginal, the combination of storage and subsequent retrieval followed by laser-induced fluorescence analysis becomes the preferred option. In particular for experiments in which one molecule of DNA combined with an *in vitro* expression system produces protein that is linked to its genotype by the droplet boundary, the amount of protein may be extremely small and thus higher sensitivity detection will be crucial to identify 'hits'.[11,48,49]

Taken together, the droplet array described in this paper combines the practical benefits of microfluidics (such as low consumption of reagents) with the strategic advantages of compartmentalization. Compartmentalization prevents cross contamination between different microreactors and provides a genotype-phenotype linkage.[48] The latter is a crucial condition to be able to evolve catalytic proteins for multiple turnover by co-compartmentalising product. Alternative methods to connect genotype and phenotype by means other than a droplet compartment that are often used for the evolution of binding proteins are less useful for selecting multiple turnover catalysts.[50]

Remobilisation of droplets after storage allows the incorporation of downstream modules such as droplet sorters.[20,23] Entrapping droplets in a simple microfluidic array provides a direct analogue to conventional well-based systems, and constitutes a novel module for chip-based enzymatic or cell-based screening systems.

The simple biological experiments described here provide a method for addressing more complex challenges in directed evolution or single cell studies in future work.

Acknowledgements

A.H. is grateful for a pre-doctoral fellowship of the Marie Curie Early Stage Training Site 'ChemBioCam'. This project was funded by the RCUK Basic Technology Programme. F.H. is an ERC Starting Investigator. The mRFP1 gene was a kind gift from the Tsien Laboratory, San Diego. Dr. Luis Olguin, Cambridge, is acknowledged for cloning the mRFP1 gene into the pIVEX construct. The galactosidase ssβG plamid was a kind gift from Prof. Benjamin G. Davis, Oxford University.

References

1 P. S. Dittrich and A. Manz, *Nat. Rev. Drug Discov.*, 2006, **5**, 210–218.
2 J. J. Diaz-Mochon, G. Tourniaire and M. Bradley, *Chem. Soc. Rev.*, 2007, **36**, 449–457.
3 D. Klenerman and Y. Korchev, *Nanomedicine*, 2006, **1**, 107–114.
4 F. d. r. Lemaire and C. l. A. Mandon, *PLoS ONE*, 2007, **2**, e163.
5 J. R. Rettig and A. Folch, *Anal. Chem.*, 2005, **77**, 5628–5634.
6 D. DiCarlo and L. P. Lee, *Anal Chem*, 2006, **78**, 7918–7925.
7 D. DiCarlo, N. Aghdam and L. P. Lee, *Anal. Chem.*, 2006, **78**, 4925–4930.
8 W.-H. Tan and S. Takeuchi, *Lab Chip*, 2008, **8**, 259–266.
9 W.-H. Tan and S. Takeuchi, *Proc. Natl. Acad. Sci. U. S. A.*, 2007, **104**, 1146–1151.
10 A. Huebner, S. Sharma, M. Srisa-Art, F. Hollfelder, J. B. Edel and A. J. deMello, *Lab Chip*, 2008, **8**, 1244–1254.
11 O. J. Miller, K. Bernath, J. J. Agresti, G. Amitai, B. T. Kelly, E. Mastrobattista, V. Taly, S. Magdassi, D. S. Tawfik and A. D. Griffiths, *Nat. Methods*, 2006, **3**, 561–570.
12 D. S. Tawfik and A. D. Griffiths, *Nat. Biotechnol.*, 1998, **16**, 652–656.
13 P. B. Umbanhowar, V. Prasad and D. A. Weitz, *Langmuir*, 2000, **16**, 347–351.
14 M. Joanicot and A. Ajdari, *Science*, 2005, **309**, 887–888.
15 F. Courtois, L. F. Olguin, G. Whyte, D. Bratton, W. T. S. Huck, C. Abell and F. Hollfelder, *ChemBioChem*, 2008, **9**, 439–446.
16 H. Song, J. D. Tice and R. F. Ismagilov, *Angew Chem., Int. Ed.*, 2003, **42**, 768–772.
17 P. S. Dittrich, M. Jahnz and P. Schwille, *ChemBioChem*, 2005, **6**, 811–814.
18 S. Koster, F. E. Angile, H. Duan, J. J. Agresti, A. Wintner, C. Schmitz, A. C. Rowat, C. A. Merten, D. Pisignano, A. D. Griffiths and D. A. Weitz, *Lab Chip*, 2008, **8**, 1110–1115.
19 D. R. Link, S. L. Anna, D. A. Weitz and H. A. Stone, *Phys. Rev. Lett.*, 2004, **92**, 054503.
20 D. R. Link, E. Grasland-Mongrain, A. Duri, F. Sarrazin, Z. Cheng, G. Cristobal, M. Marquez and D. A. Weitz, *Angew Chem., Int. Ed.*, 2006, **45**, 2556–2560.
21 L. M. Fidalgo, C. Abell and W. T. S. Huck, *Lab Chip*, 2007, **7**, 984–986.
22 C. N. Baroud, M. R. d. S. Vincent and J.-P. Delville, *Lab Chip*, 2007, **7**, 1029–1033.
23 L. M. Fidalgo, G. Whyte, D. Bratton, C. F. Kaminski, C. Abell and W. T. Huck, *Angew Chem., Int. Ed.*, 2008.
24 C. N. Baroud, J. P. Delville, F. Gallaire, R. Wunenburger, *Los Alamos National Laboratory, Preprint Archive, Physics*, 2006.
25 A. E. Sgro, P. B. Allen and D. T. Chiu, *Anal. Chem.*, 2007, **79**, 4845–4851.
26 E. M. Chan, A. P. Alivisatos and R. A. Mathies, *J. Am. Chem. Soc.*, 2005, **127**, 13854–13861.
27 H. Song and R. F. Ismagilov, *J. Am. Chem. Soc.*, 2003, **125**, 14613–14619.
28 L. S. Roach, H. Song and R. F. Ismagilov, *Anal. Chem.*, 2005, **77**, 785–796.
29 Y. C. Tan, K. Hettiarachchi, M. Siu, Y. R. Pan and A. P. Lee, *J. Am. Chem. Soc.*, 2006, **128**, 5656–5658.
30 M. He, J. S. Edgar, G. D. Jeffries, R. M. Lorenz, J. P. Shelby and D. T. Chiu, *Anal. Chem.*, 2005, **77**, 1539–1544.
31 A. Huebner, L. F. Olguin, D. Bratton, G. Whyte, W. T. S. Huck, A. J. deMello, J. B. Edel, C. Abell and F. Hollfelder, *Anal. Chem.*, 2008, **80**, 3890–3896.

32 N. R. Beer, E. K. Wheeler, L. Lee-Houghton, N. Watkins, S. Nasarabadi, N. Hebert, P. Leung, D. W. Arnold, C. G. Bailey and B. W. Colston, *Anal. Chem.*, 2008, **80**, 1854–1858.
33 B. Zheng, C. J. Gerdts and R. F. Ismagilov, *Curr. Opin. Struct. Biol.*, 2005, **15**, 548–555.
34 J. u. Shim, G. Cristobal, D. R. Link, T. Thorsen, Y. Jia, K. Piattelli and S. Fraden, *J. Am. Chem. Soc.*, 2007, **129**, 8825–8835.
35 M. Srisa-Art, A. J. deMello and J. B. Edel, *Anal. Chem.*, 2007, 6682–6689.
36 A. Huebner, M. Srisa-Art, D. Holt, C. Abell, F. Hollfelder, A. J. deMello and J. B. Edel, *Chem. Commun.*, 2007, 1218–1220.
37 D. C. Duffy, J. C. McDonald, O. J. A. Schueller and G. M. Whitesides, *Anal. Chem.*, 1998, **70**, 4974–4984.
38 G. M. Whitesides, *Annu. Rev. Mater. Sci.*, 1998.
39 S. L. Anna, N. Bontoux and H. A. Stone, *Appl. Phys. Lett.*, 2003, **82**, 364–366.
40 B. Zheng, J. D. Tice and R. F. Ismagilov, *Anal. Chem.*, 2004, **76**, 4977–4982.
41 R. E. Campbell, O. Tour, A. E. Palmer, P. A. Steinbach, G. S. Baird, D. A. Zacharias and R. Y. Tsien, *Proc. Natl. Acad. Sci. U. S. A.*, 2002, **99**, 7877–7882.
42 T. Ward, M. Faivre, M. Abkarian and H. A. Stone, *Electrophoresis*, 2005, **26**, 3716–3724.
43 J. J. Tree, G. C. Ulett, J. L. Hobman, C. Constantinidou, N. L. Brown, C. Kershaw, M. A. Schembri, M. P. Jennings and A. G. McEwan, *Environ. Microbiol.*, 2007, **9**, 2110–2116.
44 J. Clausell-Tormos, D. Lieber, J.-C. Baret, A. El-Harrak, O. J. Miller, L. Frenz, J. Blouwolff, K. J. Humphry, S. Köster, H. Duan, C. Holtze, D. A. Weitz, A. D. Griffiths and C. A. Merten, *Chem. Biol.*, 2008, **15**, 427–437.
45 T. Nagai, K. Ibata, E. S. Park, M. Kubota, K. Mikoshiba and A. Miyawaki, *Nat. Biotechnol.*, 2002, **20**, 87–90.
46 J. Cheng, J.-F. Chen, M. Zhao, Q. Luo, L.-X. Wen and K. D. Papadopoulos, *J. Colloid Interface Sci.*, 2007, **305**, 175–182.
47 J. Bibette, F. L. Calderon and P. Poulin, *Rep. Progr. Phys.*, 1999, 969.
48 H. Leemhuis, V. Stein, A. D. Griffiths and F. Hollfelder, *Curr. Opin. Struct. Biol.*, 2005, **15**, 472–478.
49 B. T. Kelly, J.-C. Baret, V. Taly and A. D. Griffiths, *Chem. Commun.*, 2007, 1773–1788.
50 H. R. Hoogenboom, *Nat. Biotechnol.*, 2005, **23**, 1105–1116.

